Spatiotemporal Air Quality Mapping and PM10 Modelling in Abu Dhabi City, UAE

Ruba El Mootassem, Zahraa Al-Dawood, and Tarig Ali*

Department of Civil Engineering, American University of Sharjah, Sharjah, United Arab Emirates
Email: g00070816@aus.edu (R.E.M.); g00074421@aus.edu (Z.A.-D.); atarig@aus.edu (T.A.)
*Corresponding author

Manuscript received August 10, 2023; revised October 26, 2023; accepted November 17, 2023; published March 8, 2024

***Abstract*—Air pollution is a global health concern that should be monitored to avoid grave consequences on human health. The rapid developments in the United Arab Emirates, in combination with its geographic location and arid climate, make it an area susceptible to unhealthy air quality indices, particularly due to the high concentrations of particulate matter in the country. Air quality can be monitored through a combination of ground data and satellite imagery. In this study, a numerical model was developed to estimate particulate matter 10 µm in size (PM10) concentrations in Abu Dhabi City through linear regression analysis using data points from 2016, 2018, and 2020. The model was validated, and the data was processed to generate PM10 concentration maps for the area of interest. The maps show similar levels of PM10, with higher unhealthy concentrations reported in desert and suburban areas. The model was validated using data from 2021, and the map reveals unhealthy concentrations across various areas in the area of interest. This study also examines the concentrations of nitrogen dioxide, sulfur dioxide, and formaldehyde in 2018 and 2020 for the same area of interest using Sentinel-5P imagery. The results show that the concentration of nitrogen dioxide decreased in 2020, likely due to imposed lockdowns and reduced industrial activities during the COVID-19 pandemic. Overall, formaldehyde and sulfur dioxide concentrations were relatively low in both years, indicating that PM10 pollution is of higher concern than other contaminants in the United Arab Emirates.**

***Keywords*—air quality mapping, particulate matter, air pollution**

I. Introduction

Air quality is an important indicator of human health and wellbeing. Any increase in the concentration of harmful pollutants can significantly impact human health, increasing risks of cardiovascular diseases, asthma, and premature deaths [1, 2]. The World Health Organization [3] estimates that 99% of the global world population are exposed to concentrations of air pollutants that exceed the guideline limits. Outdoor air pollution is estimated to have caused over 4 million premature deaths in 2019 alone [3]. Ambient air pollution may result from anthropogenic causes, natural causes, or both. Anthropogenic causes include urbanization and mass mobility (emissions from the transportation industry) while natural causes include sandstorms and wind movement (i.e., transport of pollutants through wind) [2, 4]. In the United Arab Emirates (UAE), the rapid urbanization, great number of vehicles, as well as the oil and gas industry have significantly contributed to air pollution. The location of the UAE in the Arabian Peninsula has also increased the air pollution levels in the country. Particulate matter (PM), or aerosols, are particularly rampant in the region [5, 6]. Aerosols are suspended particles in the air, and may consist of sulfates, nitrates, ammonia, salts, and dust [3]. These particles are classified by their size: 10 µm (PM10) or 2.5 µm (PM2.5). Studies have estimated that high PM10 concentrations in the UAE have resulted in 7% of the total deaths in 2007 [2].

The grave impacts of air pollution on human health make it necessary to continuously monitor the air quality to accurately examine, forecast, and enhance air quality. Ground monitoring stations monitor the concentrations of different air pollutants, such as particulate matter, ozone (O_3), carbon monoxide (CO), nitrogen dioxide (NO_2), and sulfur dioxide (SO_2). These stations, however, are limited in number, and the data provided may not be accessible to the public. Satellite imagery can be used, instead, and has been analyzed in literature to monitor the concentration of various air pollutants, NO_2 [7], and CH_4 [1], and SO_2 [8]. Satellite imagery may be combined with data from ground monitoring stations to map the air quality across an entire area [9]. The pixel properties in the satellite images include information that aids in estimating the prediction model for different geographical locations.

Despite the numerous applications for satellite images, their use in estimating pollutant concentration models is limited in literature, with only a few studies using satellite images to create these prediction models [7, 9, 10]. Different regression models have been developed in the literature to correlate data from satellite imagery to the concentration of PM [9–12]. For the UAE, an area highly susceptible to sandstorms and high aerosol concentrations, satellite images can be useful in creating models to estimate the concentration of PM to better understand the spatiotemporal behavior of aerosols across the country. Only one study has attempted to create a PM10 model for the UAE, for the city of Al Ain specifically, using MODIS Aerosol Optical Depth (AOD) data to create a linear regression model correlating the AOD to the PM10 concentration over the city [10]. Creating a correlation model between the PM10 concentrations and data contained within Landsat imagery can help in mapping the PM10 concentrations in the UAE.

There are forty-one ground monitoring stations in the UAE, nineteen of which are in Abu Dhabi [13, 14]. Abu Dhabi is particularly susceptible to sandstorms, which increases the concentration of PM10 in the air. The city is also subject to a very high rate of urbanization [4]. Therefore, it is necessary to map the air quality of the area over the years to examine the pattern of the varying concentration levels of air pollutants. The main goal of this study is to examine the air quality in the city of Abu Dhabi, the area of interest (AOI) for this project, using numerical estimates and satellite imagery. A PM10 prediction model was developed using multi-

spectral surface reflectance values from Landsat 8 Operational Land Image (OLI) imagery, which has not been examined in the literature for the UAE. The air quality in the city was further examined through assessing the levels of NO_2, SO_2, and formaldehydes (HCHO) using data obtained from Sentinel-5P. The air quality was examined across three different years: 2016, 2018, and 2020 in the month of July specifically, to assess the impact of COVID-19 lockdown restrictions on the air quality in the city. The developed numerical model estimating the PM10 concentration was validated using data from 2021.

II. Materials and Methods

A. Project Scope and Study Area

The study area for this project is Abu Dhabi, the capital city of the United Arab Emirates. Abu Dhabi is located on the northeast side of the Arabian Gulf with geographical coordinates of 24°28'0" N, 54°22'0" E. The emirate has a total area of 67,340 km², with a 600 km coastline [15]. The occurrence of sandstorms and heatwaves is common in Abu Dhabi due to its geographic location, which significantly affects air quality and visibility. In the summer months, the temperatures peak in July and August, occasionally reaching 50ºC.

The AOI defined for this project spans Abu Dhabi City, as shown in Fig. 1. The detected air pollutants encompassed in this study are PM10, HCHO, SO_2, and NO_2. The concentrations of HCHO, SO_2, and NO_2 were retrieved from Sentinel-5P. PM10 values were determined using data from ground monitoring stations and regression analyses using surface reflectance values from Landsat 8 OLI images.

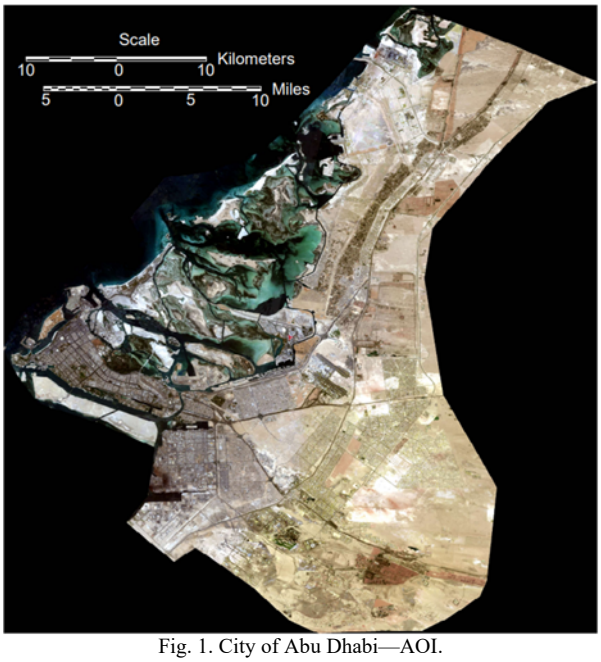

Fig. 1. City of Abu Dhabi—AOI.

B. Data Acquisition

1) Ground monitoring stations

Out of the accessible data from ground monitoring stations in Abu Dhabi, only five detect PM10 concentrations. The historical PM10 values for ground monitoring stations located in Abu Dhabi City were extracted via The Air Quality Index Visual Map website and are listed in Table 1 [16]. The PM10 concentrations detected by these stations were used to estimate the regression model.

Table 1. Locations of ground monitoring stations used in the study

Ground Monitoring Station	Longitude	Latitude
Khalifa City A	54.56917	24.42440
Khalifah High School	54.40728	24.43104
Khadija Primary School	54.36461	24.48905
US Embassy, Abu Dhabi City	54.43354	24.42533
Bain Al Jessrain	54.515588	24.40362

2) PM10—Top of Atmosphere Correlation

The Top of Atmosphere (TOA) reflectance is defined as the ratio between the reflected radiation and the incident solar radiation. Eq. (1) below represents how the TOA reflectance value is typically computed for a given band based on the digital number (DN) value in each pixel (Q_{cal}) and the relevant scaling factors (M_ρ and A_ρ) [9].

$$TOA\ reflectance = M_\rho Q_{cal} + A_\rho \quad (1)$$

Once corrected for solar angle, the TOA reflectance values for different bands can be used to calculate the aerosol optical thickness (AOT). The AOT correlates directly to PM10 concentrations, and studies in the literature have shown that a linear relationship exists between the two variables [9]. For Landsat 8 OLI imagery, the AOT can be calculated using the TOA reflectance values of the first four bands (i.e., visible bands): (1) coastal aerosol (430–450 nm), (2) blue (450–510 nm), (3) green (530–590 nm), and (4) red (640–670 nm) [17]. The relationship between TOA reflectance, AOT, and PM10 concentrations is shown in Eq. (2) and (3) below.

$$AOT = a_1B_1 + a_2B_2 + a_3B_3 + a_4B_4 \quad (2)$$

$$PM10 = a_1B_1 + a_2B_2 + a_3B_3 + a_4B_4 \quad (3)$$

where $PM10$: concentration of PM10 in μg/m^3, a_n: regression model coefficient, and B_n: atmospheric reflectance value at band n.

Google Earth Engine is a comprehensive tool for analysis of remote sensing data. The Landsat 8 TOA Reflectance Collection, available on the platform, includes corrected TOA reflectance data which can be retrieved using the code editor function. The coordinates of the ground monitoring stations were used to extract the exact reflectance values (B_n) for the first four bands, which were later used to estimate the coefficients (a_n) of the regression model. The data was extracted for the years 2016, 2018, and 2020 to create the model, and 2021 to validate the model. For consistency, the date range used was from July 20 to July 31, and the data was screened to only include images with a cloud cover of less than 10%.

3) Sentinel-5P

The Sentinel-5P satellite, which was launched from Plesetsk cosmodrome in Russia in October 2017, performs atmospheric measurements and provides data on air quality via concentrations of different air contaminants [18]. The satellite data was used in this project to extract six images as summarized in Table 2 from the AOI. The extracted maps provide information on concentrations of HCHO, SO_2, and NO_2 in July of 2018 and 2020. The images were extracted using Copernicus Open Access Hub.

Table 2. Locations of ground monitoring stations used in the study

Year	Air pollutant	Image no.	Image date
2018	HCHO	2018-07-22-00_00_2018-07-22-23_59_Sentinel-5P_HCHO_Formaldehyde	22-07-2018
2018	SO_2	2018-07-22-00_00_2018-07-22-23_59_Sentinel-5P_SO2_Sulfur_Dioxide	22-07-2018
2018	NO_2	2018-07-31-00_00_2018-07-31-23_59_Sentinel-5P_NO2_Nitrogen_Dioxide	22-07-2018
2020	HCHO	2020-07-22-00_00_2020-07-22-23_59_Sentinel-5P_HCHO_Formaldehyde	22-07-2020
2020	SO_2	2020-07-22-00_00_2020-07-22-23_59_Sentinel-5P_SO2_Sulfur_Dioxide	22-07-2020
2020	NO_2	2020-07-22-00_00_2020-07-22-23_59_Sentinel-5P_NO2_Nitrogen_Dioxide	22-07-2020

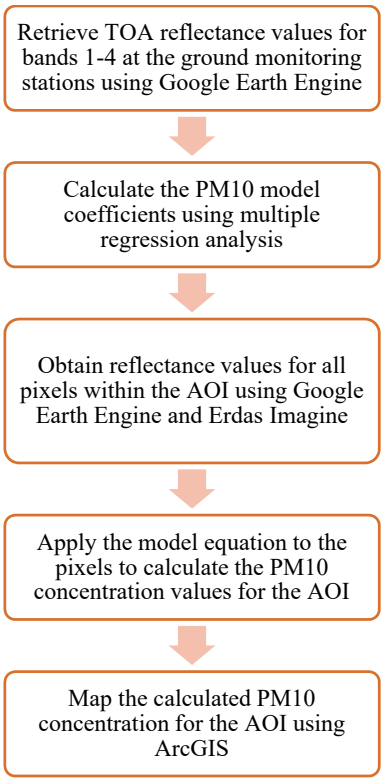

Fig. 2. Method of estimating PM10 concentration model.

C. Data Processing

1) Model creation and validation

The equations estimating the concentration of PM10 (i.e., Eq. (3)) were formed for each ground monitoring station using the detected PM10 values for each year. The system of indeterminate equations (15 equations, 4 unknown values) was solved using the multiple linear regression analysis on Excel (Data Analysis add-in). The algorithm computes the regression model coefficients by optimizing the coefficient of determination (R^2). The percentage error was also computed for each estimation at the different ground monitoring stations. The regression model was validated using reflectance data for the same ground monitoring stations for the year 2021.

2) Mapping concentrations of PM10

After verification, the model was applied to the AOI. Images in the tag image file format (TIFF) were retrieved from the Landsat 8 TOA Reflectance Collection using Google Earth Engine. These images were then opened using Erdas Imagine, and the pixel data (i.e., reflectance values for all the bands at each pixel) was exported using the Pixel to ASCII tool. The ASCII files were processed using Excel, and the estimated regression model was applied to the AOI. The calculated concentrations were then mapped using ArcGIS. Fig. 2 below summarizes the algorithm employed in estimating the numerical model.

III. Result and Discussion

A. PM10 Estimation Model

The retrieved reflectance values for each ground monitoring station are shown in Table 3. There were 15 data points in total, with an average value of 211.87 µg/m^3 and a standard deviation of 67.51 µg/m^3.

Table 3. Reflectance value for each band at each ground monitoring station

Year	Ground Monitoring Station	B_1	B_2	B_3	B_4	PM10 Concentration (µg/m^3)
2021	Khalifa City	0.257	0.261	0.28	0.311	223
	Kalifah High School	0.248	0.249	0.26	0.287	161
	Khadija Primary School	0.217	0.207	0.195	0.204	169
	US Embassy	0.234	0.23	0.234	0.251	347
	Bain Al Jessrain	0.245	0.247	0.267	0.296	193
2020	Khalifa City	0.262	0.269	0.304	0.346	197
	Kalifah High School	0.246	0.251	0.282	0.322	163
	Khadija Primary School	0.204	0.196	0.200	0.211	141
	US Embassy	0.219	0.213	0.222	0.242	117
	Bain Al Jessrain	0.250	0.255	0.293	0.343	173
2018	Khalifa City	0.238	0.239	0.259	0.293	213
	Kalifah High School	0.227	0.226	0.236	0.265	181
	Khadija Primary School	0.206	0.194	0.191	0.201	205
	US Embassy	0.213	0.205	0.211	0.229	199
	Bain Al Jessrain	0.227	0.223	0.240	0.273	189
2016	Khalifa City	0.248	0.253	0.280	0.319	317
	Kalifah High School	0.243	0.247	0.268	0.305	275
	Khadija Primary School	0.203	0.193	0.195	0.201	299
	US Embassy	0.215	0.208	0.217	0.235	149
	Bain Al Jessrain	0.232	0.236	0.261	0.305	360

The final model, estimated using multiple linear regression analysis, is shown in Eq. (4) below:

$$PM10 = -7016.41B_1 + 15013.8B_2 - 8708.34B_3 + 1944.9B_4 \quad (4)$$

The R^2 value was determined to be 0.808, indicating a strong correlation and a robust model. Saraswat *et al*. [9] also estimated a strong model with a high R^2 value. Their study, however, was limited to one time period only, as opposed to three. Saleous *et al.* [10] similarly estimated a model with a regression value of 0.75 for Al Ain.

The study was validated using the data from the ground monitoring stations in 2021 and the data from the years used in the creation of the model, as shown in Table 4 below. Overall, the model was the most accurate in predicting the PM10 concentration for 2018 but was not as accurate in predicting the PM10 concentrations for 2021.

Table 4. Predicted PM10 values at the ground monitoring stations.

Year	Ground Monitoring Station	Predicted PM10 concentration (μg/m^3)	% Difference	Date
2021	Khalifa City	281.9	26.42	July 24
	Kalifah High School	292.4	81.60	
	Khadija Primary School	283.9	68.00	
	US Embassy	261.7	24.57	
	Bain Al Jessrain	239.9	24.32	
2020	Khalifa City	226.0	16.31	July 21
	Kalifah High School	212.9	11.84	
	Khadija Primary School	180.1	43.44	
	US Embassy	198.8	6.04	
	Bain Al Jessrain	190.0	55.01	
2018	Khalifa City	232.8	4.76	July 23
	Kalifah High School	260.6	24.10	
	Khadija Primary School	194.9	6.83	
	US Embassy	191.3	13.99	
	Bain Al Jessrain	196.3	47.28	
2016	Khalifa City	240.5	23.92	July 26
	Kalifah High School	262.8	7.63	
	Khadija Primary School	166.1	18.30	
	US Embassy	181.7	13.32	
	Bain Al Jessrain	235.8	59.93	

The equation was applied to the AOI to map the PM10 concentrations across the city. It is worthwhile to mention that dust storms are more common during the summer in the UAE, hence why high PM10 values are typically observed during summer seasons compared to other seasons [5, 6]. In other studies, the PM10 values were observed to substantially decrease between the months of October to April in the UAE [10, 14]. This may mean that the model estimated in this paper will not accurately predict the PM10 concentrations for different seasons.

B. PM10 Concentration Map

Fig. 3 below shows the mapped concentration levels for the AOI. The maps show the unhealthy PM10 concentrations (exceeding 255 μg/m^3, resulting in an air quality index exceeding 150) and moderate PM10 concentrations (less than 155 μg/m^3, resulting in an air quality index of less than 100).

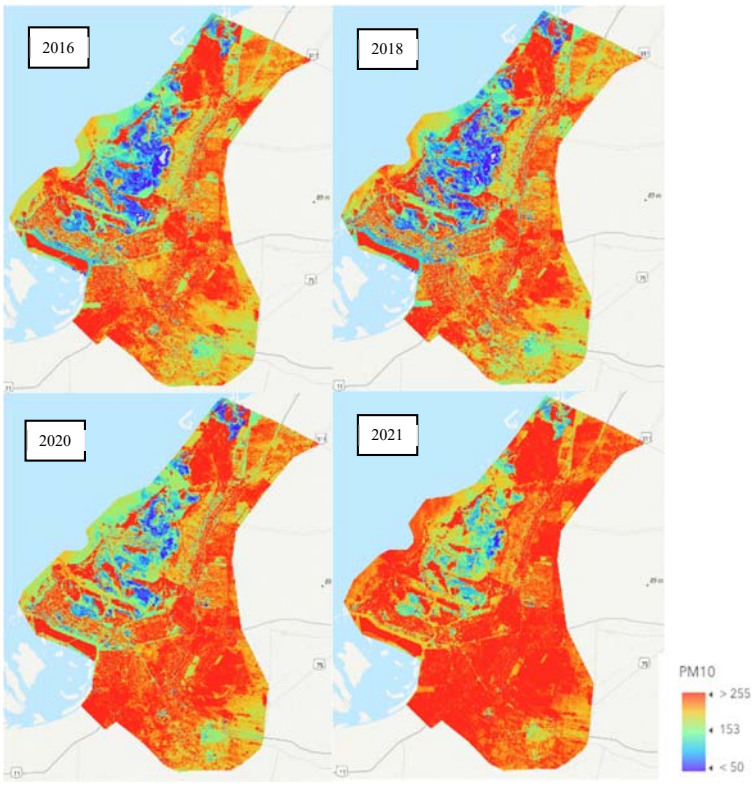

Fig. 3. PM10 map for the AOI.

Overall, all maps show a similar trend, with desert and suburban areas (areas further away from the Arabian Gulf) showing greater concentrations of PM10 than urban areas, affirming that the high concentrations of PM10 characteristic of the region are caused primarily by natural conditions and frequent sandstorms. Urban areas further from the desert and suburban areas, and closer to the Arabian Gulf, show lower PM10 concentrations, consistent with studies in the literature [14]. The lowest PM10 concentrations are reported over Khor Laffan, the creek, and the surrounding islands. The 2020 map shows concentration levels similar to the preceding years, indicating that COVID-19 lockdown restrictions had no impact on the PM10 concentrations in urban areas. Incidentally, on the 21st of July of 2020, a sandstorm struck the country, with high wind speeds facilitating the transport of the aerosols over the city, and the unhealthy concentrations reported can be attributed to this storm [19, 20]. The prediction map for 2021, on the other hand, reveals that the PM10 concentration is unhealthy across almost the entire city, including urban areas However, it is worthwhile to reiterate that the estimated model was not as accurate in predicting the PM10 concentrations measured by the ground monitoring stations for 2021.

The results show that the data contained within Landsat 8 OLI imagery can provide information on the PM10 concentration over an area. The generated maps can forecast the PM10 concentrations in areas with no detection stations or real-time data, allowing for a better understanding of the pattern of the concentrations across the AOI and identifying risk-areas where the PM10 levels are unhealthy or hazardous. The PM10 regression model can also be used to observe the changes in PM10 concentrations with time across the AOI to note any particular trends and to observe the impact of global warming on the aerosol concentration.

While the estimated model has a high coefficient of determination, it is necessary to acknowledge the limitations in the model. The ground monitoring stations used in the study are stationed in urban areas relatively close to each other, thus providing a limited coverage of the detected PM10 concentrations in the AOI. The PM10 concentration values recorded by ground monitoring stations in suburban areas were inaccessible and could not be included in the model. It is important to note that the PM10 values measured by ground monitoring stations only reflect the conditions on the near surface, unlike the images captured by the satellites [10]. Additionally, natural events like sandstorms are not consistent, so the estimated model would need to be regularly updated with data to account for yearly variations.

C. Maps of Other Pollutants

Six images were extracted from Sentinel-5P to determine the concentrations of NO_2, SO_2, and HCHO in 2018 and 2020. Since the satellite was launched in 2017, images from 2016 were not available.

The NO_2 concentrations are displayed in Fig. 4. NO_2 is emitted from various sources, including power plants and industrial processes, but is mainly emitted from vehicles, and so the concentration of NO_2 over an AOI is related to the mass mobility in that area [1, 8]. In the Gulf region, specifically, NO_2 concentrations are primarily emitted from vehicles since the industrial activities in the region are minimal [8]. As seen in the maps, the NO_2 concentrations appear significantly lower in 2020, and the decrease noted further emphasizes that the higher levels observed in 2018 are related to the transportation activities in the city. This observation can be attributed to the reduced mobility of residents due to the strict lockdown measures in Abu Dhabi, which include remote working requirements, entry restrictions, and imposed curfews, effectively decreasing the mobility. Similar results were reported in other cities in the UAE and across the Middle East [1, 8, 21], with COVID-19 restrictions proving effective in decreasing the concentrations of NO_2.

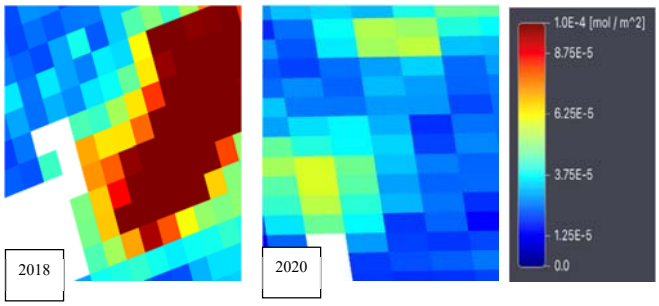

Fig. 4. Sentinel-5P images for NO_2 concentrations.

Fig. 5 presents the concentrations of HCHO, a carcinogenic gas produced from various sources, including open biomass burning, vehicles, and other photochemical reactions in the atmosphere [22, 23]. Concentrations of HCHO over Abu Dhabi city are generally low for both years, and the highest concentration observed was approximately 3.75E-5 mol/m^2 in 2018. Mapping concentrations of HCHO over an AOI is an area that is not studied extensively in the literature, particularly for this region, despite the severely harmful effects of the gas [23]. Similar to NO_2, HCHO concentrations are lower in 2020 than 2018. SO_2 concentrations, shown in Fig. 6, also appear lower in 2020 than 2018 but are relatively low in both years. SO_2 gas is typically produced from burning of fossil fuels, from ships and locomotives, or from industrial processes [21]. Other studies have also observed a decrease in the concentration of SO_2 in the wake of lockdown measures, but not as much as that observed for NO_2 [8].

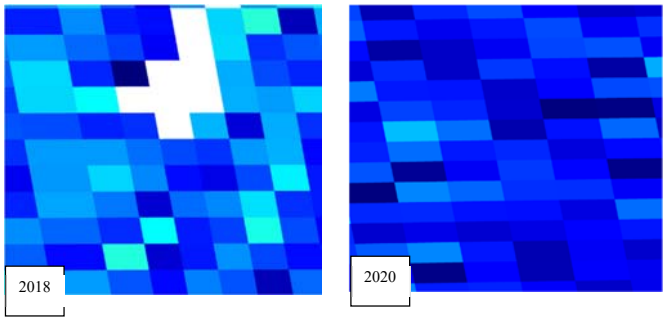

Fig. 5. Sentinel-5P images for HCHO concentrations.

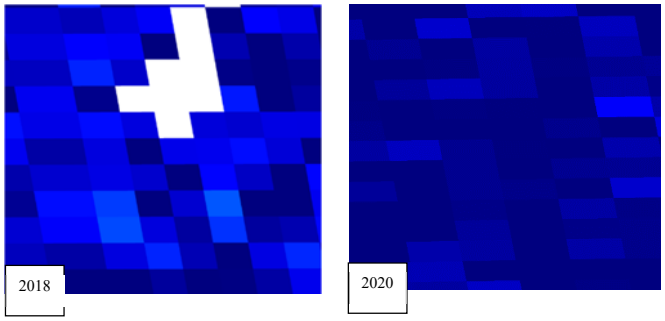

Fig. 6. Sentinel-5P images for SO_2 concentrations.

IV. Conclusion

This study examined the air quality in Abu Dhabi city using satellite imagery and numerical models to map the concentration of various air pollutants, including HCHO, SO_2, NO_2, and PM10. The concentrations of HCHO, SO_2, and NO_2 were determined using Sentintel-5P imagery while the PM10 concentrations were estimated using a multiple regression model correlating the TOA reflectance values in the visible bands in Landsat 8 imagery to data from ground monitoring stations. The Sentinel-5P images show that the concentration of NO_2 decreased in 2020 relative to 2018, likely due to the COVID-19 lockdown restrictions, while the concentrations of SO_2 and HCHO were similar in both years. The regression coefficients of the PM10 model were calculated using data from the years 2016, 2018, and 2020, and the R^2 value was determined to be 0.808. The developed model was used to map the concentrations of PM10 across the AOI for the years 2016, 2018, 2020, and 2021 for a better understanding of the PM10 concentrations in areas with no monitoring stations. The results show that the concentrations of PM10 were similar in 2016, 2018, and 2020. The results also show that suburban and desert areas have greater PM10 concentrations compared to urban areas. The forecasted map for 2021 revealed unhealthy levels of PM10 across the AOI, but the predicted concentration values at the ground monitoring stations were less accurate compared to the preceding years. To improve the accuracy of the model, data from suburban and desert areas, which were not accessible for this study, should be included to expand the coverage of the model. Future work can focus on developing PM10 maps using the same algorithm to observe the trends in the changes in PM10 concentrations over longer periods of time across Abu Dhabi city. Future studies can also look into developing PM10 models in other months of the year to understand the seasonal patterns in the concentration across the AOI.

Conflict of Interest

The authors declare no conflict of interest.

Author Contributions

R.E.M: conceptualization, retrieval of data, analysis of results, writing the paper, revisions; Z.A.D: conceptualization, retrieval of data, analysis of results, writing the paper, revisions; T. A. – conceptualization, supervision, revisions; all authors had approved the final version.

References

[1] A. Shanableh, R. Al-Ruzouq, K. Hamad, M. B. Gibril, M. A. Khalil, I. Khalifa, Y. El Traboulsi, B. Pradhan, R. Jena, S. Alani, M. Alhosani, M. H. Stietiya, M. Al Bardan, and S. AL-Mansoori, "Effects of the COVID-19 lockdown and recovery on people's mobility and air quality in the United Arab Emirates using satellite and ground observations," *Remote Sensing Applications: Society and* Environment, vol. 26, 100757, 2022.

[2] Y. Li, J. M. Gibson, P. Jat, G. Puggioni, M. Hasan, J. J. West, W. Vizuete, K. Sexton, and M. Serre, "Burden of disease attributed to anthropogenic air pollution in the United Arab Emirates: Estimates based on observed air quality data," *Science of The Total Environment*, vol. 408, no. 23, pp. 5784–5793, 2010.

[3] World Health Organization. Ambient (outdoor) Air Pollution. [Online]. Available: https://www.who.int/news-room/fact-sheets/detail/ambient-(outdoor)-air-quality-and-health

[4] A. Abuelgasim and A. Farahat, "Effect of dust loadings, meteorological conditions, and local emissions on aerosol mixing and loading variability over highly urbanized semiarid countries: United Arab Emirates Case Study," *Journal of Atmospheric and Solar-Terrestrial Physics*, vol. 199, 105215, 2020.

[5] A. Barbulescu and Y. Nazzal, "Statistical analysis of dust storms in the United Arab Emirates," *Atmospheric Research*, vol. 231, no. 1, 104669, 2020.

[6] A. Abuelgasim, M. Bilal, and I. A. Alfaki, "Spatiotemporal variations and long-term trends analysis of aerosol optical depth over the United Arab Emirates," *Remote Sensing Applications: Society and Environment*, vol. 23, 100532, 2021.

[7] A. Al Yammahi and Z. Aung, "Forecasting the concentration of NO_2 using statistical and machine learning methods: A case study in the UAE," *Heliyon*, vol. 9, no. 2, E12584, 2023.

[8] A. M. El Kenawy, J. I. Lopez-Moreno, M. F. McCabe, F. Dominguez-Castro, D. Pena-Angulo, I. M. Gaber, A. S. Alqasemi, K. M. Al Kindi, T. Al-Awadhi, M. E. Hereher, S. M. Robaa, N. Al Nasiri, and S. M. Vicente-Serrano, "The impact of COVID-19 lockdowns on surface urban heat island changes and air-quality improvements across 21 major cities in the Middle East," *Environmental Pollution*, vol. 288, 117802, 2022.

[9] I. Saraswat, R. K. Mishra, and A. Kumar, "Estimation of PM10 concentration from Landsat 8 OLI satellite imagery over Delhi, India," *Remote Sensing Applications: Society and Environment*, vol. 8, pp. 251–257, 2017.

[10] N. Saleous, S. Issa, and M. Alsuwaidi, "Using modis aerosol optical depth to predict PM10 over Al Ain region, UAE," *The International Archives of the Photogrammetry, Remote Sensing and Spatial Information Sciences*, pp. 419–423, 2021.

[11] J. Wang and S. A. Christopher, "Intercomparison between satellite-derived aerosol optical thickness and PM2.5 mass: Implications for air quality studies," *Atmospheric Science*, vol. 30, no. 21, 2003.

[12] N. Othman, M. Z. Mat Jafri, H. S. Lim, and K. Abdullah, "Satellite retrieval of aerosol optical thickness over arid region: Case study over Makkah, Mina and Arafah, Saudi Arabia," *Journal of Applied Sciences*, vol. 10, pp. 3021–3031, 2010.

[13] Ministry of Climate Change and Environment. *Air Quality Index Manual.* [Online]. Available: https://www.moccae.gov.ae/assets/91c95f18/uae-air-quality-index-manual.aspx

[14] A. Abuelgasim and A. Farahat, "Investigations on PM10, PM2.5, and their ratio over the Emirate of Abu Dhabi, United Arab Emirates," *Earth Systems and Environment*, vol. 4, pp. 763–775, 2020.

[15] Abu Dhabi Geography. [Online]. Available: https://www.abudhabi.com/v/geography/

[16] IQAIR. Air Quality in United Arab Emirates. [Online]. Available: https://www.iqair.com/united-arab-emirates

[17] United States Geological Survey. *Landsat 8, Landsat Missions.* [Online]. Available: https://www.usgs.gov/landsat-missions/landsat-8

[18] The European Space Agency. *Sentintel-5P.* [Online]. Available: https://sentinels.copernicus.eu/web/sentinel/missions/sentinel-5p

[19] Gulf News. UAE weather: Beware! There's a sandstorm in the UAE. [Online]. Available: https://gulfnews.com/uae/weather/uae-weather-beware-theres-a-sandstorm-in-the-uae-1.1595331530584?slide=1

[20] The National. Powerful sandstorm and rain strike Abu Dhabi. [Online]. Available: https://www.thenationalnews.com/uae/environment/powerful-sandstorm-and-rain-strike-abu-dhabi-1.1053200

[21] Y. O. Kaied, A. S. K. Darwish, and P. Farrell, "COVID-19 impact on air quality and associated elements: Knowledge data of the Emirate of Ajman—UAE," *Renewable Energy and Environmental Sustainability*, vol. 6, 2021.

[22] C. Zhang, J. Li, W. Zhao, Q. Yao, H. Wang, and B. Wang, "Open biomass burning emissions and their contribution to ambient formaldehyde in Guangdong province, China," *Science of the Total Environment*, vol. 838, no. 1, 155904, 2022.

[23] S. Qiu, Z. He, G. Liu, Z. Ding, Z. Bu, J. Cao, W. Ji, W. Liu, C. Su, X. Wang, F. Liu, F. Li, F., T. Li, H. Qian, and C. Liu, "Ambient formaldehyde concentrations in summer in 30 Chinese cities and impacts on air cleaning of built environment," *Energy and Built Environment*, 2023.